

Uniaxial and biaxial hot pressing of PVDF films: A pathway toward high-performance piezoelectric sensors and energy harvesters

Suprpto^{1*}, Jubaidah², Selamat Triono¹, Hariyanto Gunawan³, Lisyanto¹, Aditya Sukma Nugraha⁴ and Yopan Rahmad Aldori⁵

¹ Department of Mechanical Engineering, Universitas Negeri Medan, **Indonesia**

² Department of Physics, Universitas Negeri Medan, **Indonesia**


³ Department of Mechanical Engineering, Chung Yuan Christian University, **Taiwan**

⁴ National Research and Innovation Agency (BRIN), **Indonesia**

⁵ Department of Mechanical Engineering, Universitas Medan Area, **Indonesia**

*Corresponding Author: suprpto@unimed.ac.id

Received: 01 September 2025; *Revised:* 24 January 2026; *Accepted:* 19 February 2026

 **Cite this** <https://doi.org/10.24036/teknomekanik.v9i1.44972>

Abstract: The piezoelectric efficiency of Poly (vinylidene fluoride) (PVDF) membranes becomes restricted by the challenge of generating and stabilizing electroactive β -phase during processing. Stretching requires control of deformation parameter, while solvent-based methods bring environmental and occupational health risks. This research suggests hot-pressing as an alternative method for enhancing β -phase fraction, utilizing multidirectional stress without solvent or chemical exposure. This study systematically compares uniaxial hot-pressing (Uniaxial HP) and biaxial hot-pressing (Biaxial HP) setups to determine which stress distribution is more effective at promoting changes and improving piezoelectric properties in PVDF membranes. The main objective of this research is to systematically evaluate and compare the impacts of uniaxial and biaxial hot-pressing on the crystalline phase transformation and electromechanical performance, including the piezoelectric coefficient (d_{33}) and output voltage response of PVDF membranes. PVDF pellets were hot-pressed at 220° C under a pressure of 60 MPa for 15 minutes followed by rapid quenching in ice water. X-Ray diffraction (XRD) and Fourier transform infrared spectroscopy (FTIR) confirmed phase composition, correlated with performance via the piezoelectric coefficient (d_{33}), and assessed piezoelectric activity. Experimental results show that biaxial loading provides a higher β -phase fraction (50.47%) compared to untreated membranes (47.80%) and UHP samples (49.30%). The crystallinity and the piezoelectric coefficient also increased to 49% and 18.8 pC/N, respectively. Biaxial stress pattern during hot-pressing induces favourable thermodynamic and kinetic conditions for β -phase expansion. Beyond phase-related results, the approach delivers competitive piezoelectric effectiveness while maintaining simplicity and reducing solvent-dependent processing steps.

Keywords: PVDF; uniaxial and biaxial; hot press; piezoelectric

1. Introduction

Poly(vinylidene fluoride) (PVDF) is a dielectric polymer known for its electroactive phases (α , β , γ , δ , ϵ), which depend strongly on processing conditions [1],[2]. Among these, the β -phase is most critical due to its high polarization and superior piezoelectric performance. PVDF has gained wide attention for applications in sensors, actuators, and energy harvesting systems because of its mechanical strength, thermal stability, flexibility, and ease of processing [3],[4],[5]. Previous studies reported that mechanical stretching [6], [7], high-pressure compression [8], [9], and electrical poling under high voltage [10] can increase β -phase content. However, stretched PVDF films often show limited thermal stability, and solvent casting without post-treatment yields insufficient β -

phase. Fig.1(a) presents a representative application of PVDF films in piezoelectric devices, whereas Fig.1(b) summarizes fabrication approaches employed to promote phase transformation during PVDF processing.

PVDF has become a fundamental material in the advancement of value arising from its exceptional piezoelectric capabilities, which are determined by its polymorphism. The electroactive β -phase of PVDF, distinguished by an all-trans (TTTT) molecular conformation, is the most desired for optimal sensing and energy conversion, despite the existence of several crystalline forms [4]. Nonetheless, obtaining a substantial β -phase fraction is a drawback, as the non-polar α -phase exhibits greater thermodynamic stability during conventional processing methods, such as solvent casting at ambient temperature [11], [12]. However, the conventional technique for facilitating the α -phase to β -phase transformation encompasses mechanical stretching and high-voltage poling [10], [13], [14]. Being effective, these approaches frequently yield membranes with inadequate piezoelectric intensity or insufficient thermal stability when subjected simply to uniaxial or biaxial stretching [6], [7]. Recent improvements have studied specialized fabrication methods, including intra-porous fibres for sensor and environmentally green vapor treatments to enhance membrane properties [4], [15], [16].

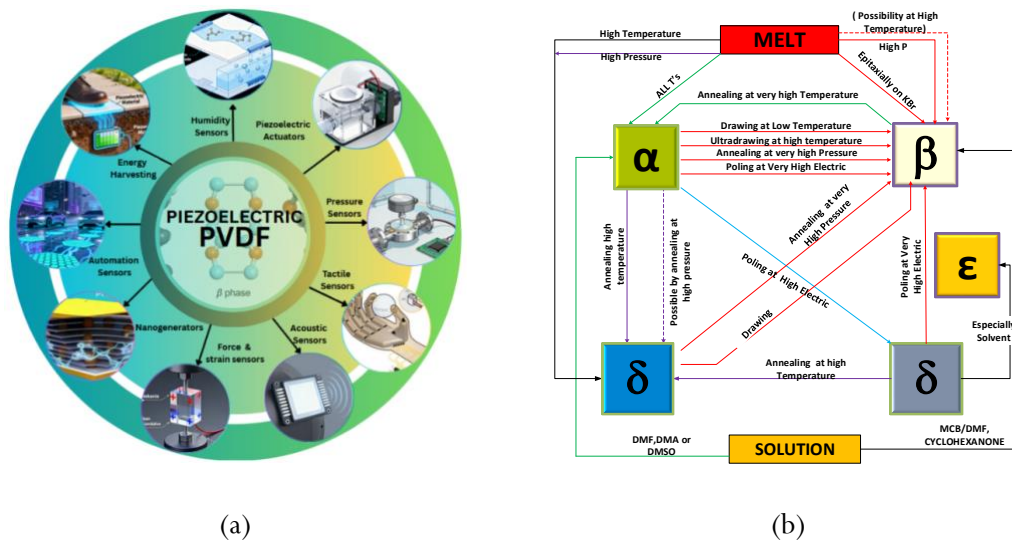


Figure 1. (a) Representative application of PVDF film in piezoelectric devices, and (b) Phase transformation methods for PVDF processing [2]

Hot pressing (HP) has been identified as a viable alternative. Through systematically manipulating the interplay between elevated pressure and temperature, HP can boost structural uniformity, diminish porosity, and drastically promote dielectric and energy storage properties [8], [9], [17]. Although it has potential, the utilization of HP requires precise optimization, as excessive heat or mechanical stress may lead to the degradation of molecular mass and chemical bonds [13], [18]. However, recent studies have shown that uniaxial compression can efficiently produce high β -phase fraction of PVDF membranes [19], and HP treatments on membranes or films have demonstrated encouraging crystalline phase transitions [8]. Nonetheless, there is a notable deficit of comparative studies examining the essential distinctions between uniaxial and biaxial HP arrangements. Biaxial stretching is recognized for its impact on the mechanical anisotropy of PVDF. However, a systematic comparison with uniaxial techniques, particularly regarding surface morphology, crystallinity, and the ensuing piezoelectric response in pure PVDF, has not yet been thoroughly investigated. This research fills a significant research void by conducting a thorough examination of the effects of uniaxial compared to biaxial HP on solvent casting of pure PVDF membranes/films. In contrast to previous studies that rely on additives to enhance the β -phase formation, we

demonstrate that biaxial HP techniques are more feasible, scalable, and additive-free for generating dense and uniform β -phase structures. This study provides a method for developing high-performance PVDF films by investigating the evolution of crystalline phases and surface characteristics, intended for advancing wearable sensors and other devices.

2. Material and methods

Commercial PVDF pellets (Kynar PVDF®740, Arkema, Mw = 180,000, MFR = 1.1 g/10 min, specific gravity 1.78 g/cc, average size 0.5×4 mm) were used as raw materials. The pellets were dried in an oven at 50–75 °C for 30 min prior to processing. HP was performed at 220°C and 60 MPa using a stainless-steel mold ($30 \times 50 \times 15$ mm). Uniaxial hot-pressed films were prepared with dimensions of 15×15 mm, while biaxial hot-pressed films measured 15×15 mm. Cooling was carried out inside the mold to room temperature to maintain structural integrity. Film thickness varied depending on pellet mass and mold size. Each sample was fabricated in triplicate to ensure reproducibility.

2.1 Preparation of PVDF films by uniaxial and biaxial pressing

The experiments were performed using the hot press method shown in Figure 2. PVDF pellets were dried in an oven at 50-75°C for 30 minutes before pressing. The pellets were melted at 180°C for approximately 50 minutes on a flat plate heater. The molten PVDF was then inserted into a stainless-steel Mold (dimension: 30 x 50 x 15 mm), which could be pressed between the hot plates of a hydraulic press machine. The HP machine melted the PVDF pellets while forming the material uniformly. The PVDF pellet was pressed into the stainless-steel Mold at a pressure of 60 MPa. The pressure exerted on the pellets and the mold design are the primary variables that can significantly influence the final thickness of the PVDF membrane. After taking off, the membrane is prepped for biaxial HP at 15 x 15 mm and for uniaxial HP at 15 x 30 mm. The thickness of the PVDF films was measured using a digital micrometre (Elcometer 456 model EF1, London, Britain) at five different positions for each sample to ensure uniformity. The thicknesses of UHP, uniaxial HP, and biaxial HP samples were documented as $1500 \mu\text{m} (\pm 1.00 \mu\text{m})$, $450 \mu\text{m} (\pm 1.00 \mu\text{m})$, and $330 \mu\text{m} (\pm 1.00 \mu\text{m})$, respectively. The high-pressure compression process was performed at 60 MPa and 220°C for both uniaxially and biaxially pressed samples. Finally, the PVDF samples were cooled inside the press Mold until they reached room temperature.

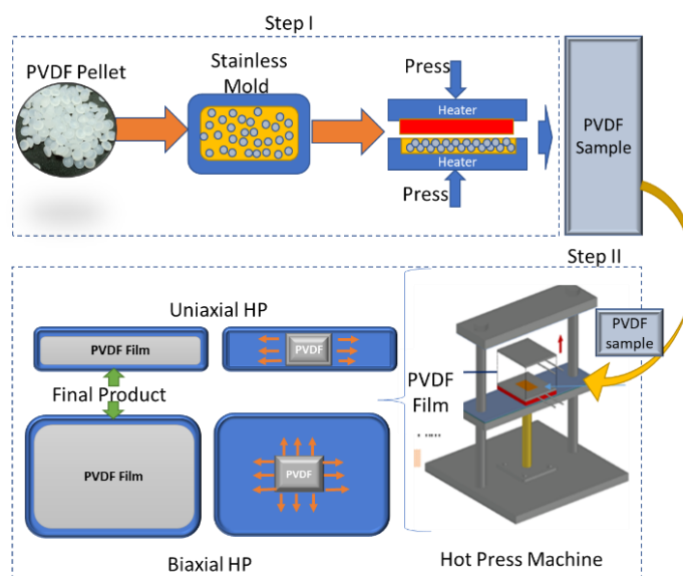


Figure 2. Schematic of the fabrication of PVDF film by Hot Pressing (HP)

2.2 Characterization and measurements

The crystalline phases of PVDF processed by uniaxial HP and biaxial HP were investigated using FTIR spectroscopy (Jasco FTIR-5000, Tokyo, Japan) in the wavenumber range of 600–1500 cm^{-1} . The fraction of the electroactive β -phase was estimated based on the characteristic absorption bands of the α and β phases. The crystal structure and degree of crystallinity were analyzed using X-ray diffraction (XRD, Siemens D5000 Diffractometer, German) with Cu-K α radiation ($\lambda = 1.54 \text{ \AA}$), collected over a 2θ range of 5° – 80° with a step size of 0.02° . The output voltage was measured using an impact-force test to assess the piezoelectric properties.

2.3 Output voltage response

The piezoelectric coefficient (d_{33}) is used as a performance index for PVDF film, which is measured using an impact force test [13], [20]. The drop impact tests are illustrated in Figure 2(a). A steel ball with a diameter of 0.018 m and a mass of 0.0237 kg is dropped from a height of 0.015 m onto the surface of the PVDF sensor sample, which has been coated with silver ink as the electrode. A guide plastic tube was used to keep the steel ball's direction perpendicular to the PVDF surface. Energy transformation occurs when the potential energy of a steel ball is converted into kinetic energy upon impact; the impact energy can be calculated to be 3.49 mJ, which is used to measure the piezoelectric coefficient (d_{33}) from the output voltage generated. As shown in Fig. 3, a thin layer of silver ink was coated on the top and bottom surfaces of the pressed PVDF film as an electrode layer and wiring system for electrical response measurements.

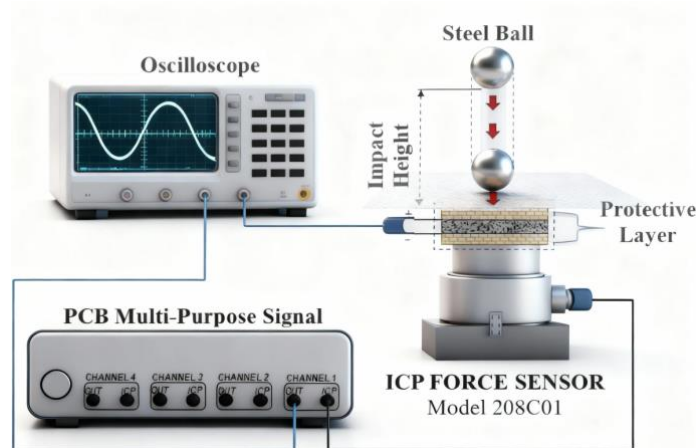


Figure 3. The schematic of the setup impact force method for measuring the output voltage and Piezoelectric coefficient (d_{33}) based on the principle of energy conversion [13]

The piezoelectric coefficient (d_{33}) along the poling direction can be calculated by [7].

$$d_{33} = \frac{Q}{F_i} = \frac{C \times V}{F_i}, \text{ where } C = \epsilon_r \epsilon_0 \frac{A}{t} \quad (1)$$

where Q represents the direct charge measurements which are obtained from direct charge measurement by recording the voltage drop across a known shunt resistor R_L to determine the Current $I(t) = V_R(t) / R_L$. The total charge is then calculated as: $Q = \int I(t) dt$; Here, F_i represents the applied force on the sample measured using an inline force sensor, from which the force–time history $F(t)$ is obtained and the peak force F_{peak} is extracted. C is the capacitance of the PVDF film; V is the measured output voltage response; ϵ_r is relative permittivity with a value of 12; ϵ_0 ($8.854 \times 10^{-12} \text{ F/m}$) is the permittivity of free space; A is the effective surface area of the electrode with width (w) = 10 mm and length (l) = 15 mm; t is the film thickness.

3. Results and discussion

XRD is used to determine and characterize the diffraction planes of α and β phases, and to assess crystal orientation in the PVDF sample, as shown in Fig.4. It can be observed that PVDF UHP showed a less intense peak than PVDF uniaxial and biaxial hot-pressing. The results are almost the same as the previous work [13], [21] that mentioned that PVDF with a monoclinic structure of α -phase was found in two intense peaks at positions of $2\theta = 18.13$ (100), 18.83 (021) and 20.86 (020). On the other hand, two peaks of β -phases were found at 27.86 and 39.18 relative to diffractions in planes (111), (021), and (002), respectively. The phase of UHP PVDF is controlled by a β -phase. In addition, the fraction of β -phase presents a superposition of peaks at 20.86 corresponding (110) crystalline plane. Samples of PVDF were prepared by uniaxially and biaxially hot-pressing, and the presences of α and β -phase have different peak intensity positions around $2q = 17.52$ to 20.13° , corresponding to diffractions in crystalline planes (020) and (200), respectively. For the sample with uniaxial HP, the peaks at $2q = 17.52^\circ$ (020), 18.22° (021), 26.47° (021), and 38.58° (002) corresponded α -phase, and 20.00° (110, 200) for β -phase. Meanwhile, the sample with biaxial HP shows the characteristics of α and β -phases similar to the uniaxial HP, as well as the peaks at $2q = 17.82^\circ$ (100), 18.58° (100), 26.47° (021), 39.03° (021). It is suggested that this was caused by the rearrangement of the PVDF macrostructure in the crystalline phase at high temperature and pressure. The enhancement of the β -phase in biaxial HP is attributed to the multi-directional mechanical stress that induces molecular chain stretching along two axes. This biaxial deformation facilitates the rotation of the C-F dipoles more effectively than uniaxial stress, forcing the polymer chains to transition from the coiled TGTG' (α) to the extended TTTT (β) conformation [7], [8]. In contrast to UHP samples, where chains exhibit random orientation, the biaxial stress distribution provides the requisite energy to overcome steric hindrance, thereby facilitating dipole alignment. This, in turn, results in enhanced crystallinity and augmented piezoelectric activity.

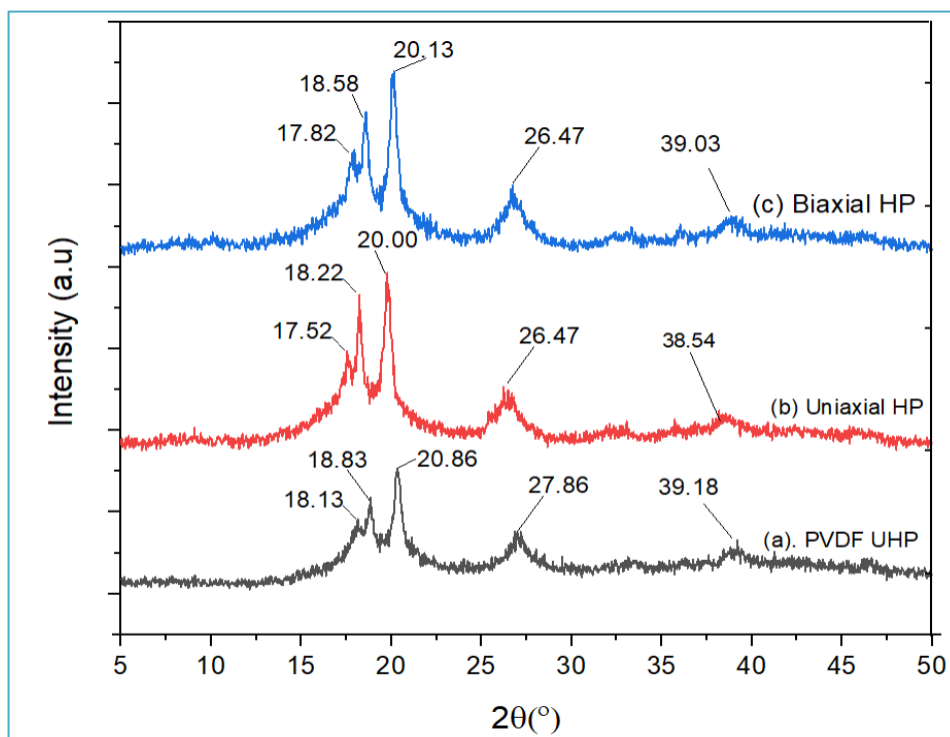


Figure 4. XRD spectra of the PVDF film (a) PVDF UHP (b) Uniaxial HP (c) Biaxial HP

Table 1 shows the diffraction of crystal planes α and β for each sample of PVDF UHP, uniaxial, and biaxial HP, and compares with previous studies.

Table 1. Diffraction Crystal Plane and angles of different phases for UHP, Uniaxial HP and Biaxially HP of PVDF Film

Hot Press Method	α		β		α		β	
	2θ (°)	Crystal plane	2θ (°)	Crystal plane	2θ (°)	Crystal plane	2θ (°)	Crystal plane
Present Study					Reference [6], [13], [22], [23]			
PVDF	18.13	(100)						
UHP	18.83	(021)	20.86	(110)				(110)
	27.86	(111)		(200)	17.66,			(200)
	39.18	(002)			18.30,	(100)		(110)
	17.52	(020)			19.90,	(020)	20.10	(200)
	18.22	(021)				(110)	20.26	(110)
Uniaxial-HP	19.77	(110)	20.00	(110)	26.56,	(021)	20.70	(200)
	26.47	(021)		(200)	27.80,	(111)	20.80	(110)
	38.54	(002)			35.70,	(200)	20.90	(200)
	17.82	(020)				(002)	36.60	(110)
Biaxial-HP	18.58	(021)	20.13	(110)	39.00.			(200)
	26.47	(111)		(200)				(020)
	39.03	(002)						(101)

3.1 Degree of crystallinity

To determine the level of crystallinity index (X_c) and the fraction of α and β phases PVDF in the sample, the XRD peaks were fitted by using Gaussian curves of Origin Pro Software as shown in figure 5. The degree of crystallinity is defined as the ratio of crystalline peaks + crystalline amorphous peaks. The degree of crystallinity was calculated using equation (2) [24]:

$$\text{Degree of crystallinity } (X_c) = \frac{S_c}{S_c + S_a} \times 100\% \quad (2)$$

where S_c and S_a represent the sum of areas of the crystalline planes and amorphous peaks in XRD diffraction peaks, respectively.

Degree of crystallinity (X_c) for all PVDF samples processed by unhot-pressing, uniaxial and biaxial HP is summarized in table 2. Compared with the unhot-pressing sample, the uniaxial and biaxial HP PVDF samples exhibit slightly higher crystallinity. The increase in PVDF crystallinity after HP is due to thermally activated chain mobility combined with pressure-assisted molecular packing. At high temperature, mobility promotes the rearrangement of PVDF chain segments from disordered amorphous regions to ordered crystalline lamellae. High pressure simultaneously reduces free volume and strengthens intermolecular interactions, leading to denser chain packing [25], [26]. This mechanism primarily promotes the growth and perfection of pre-existing crystallites, rather than facilitating extensive grain recrystallization. The result is a moderate yet consistent increase in crystallinity, typical of PVDF annealing, rather than simple melt recrystallization. To maintain the crystal domain and reduce lattice defects, optimal HP variable setting promotes the densification of the polymer matrix. While the entire degree of crystallinity is the same, the enhancement of crystal and molecular orientation is major significance [27]. The rise of piezoelectric properties is due to structural improvements that favour the β -phase and facilitate effective dipolar alignment [1].

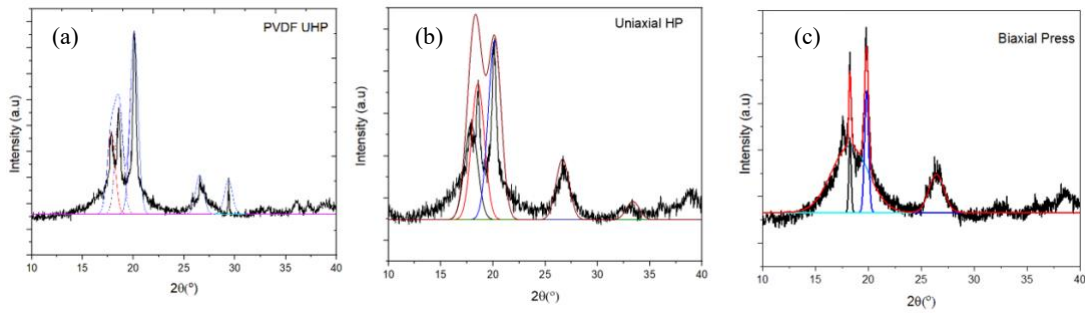


Figure 5. XRD fitted spectra: (a) UHP, (b) uniaxial HP, and (c) biaxial HP

Table 2. Degree of crystallinity calculated crystalline and amorphous peak

No	Process	Degree of crystallinity (%)
1	PVDF UHP	45
2	PVDF Uniaxial HP	48
3	PVDF Biaxial HP	49

3.2 Fast Transform Infrared Spectroscopy (FTIR)

FTIR analysis was carried out in the range of 600~1500 with a resolution of 1 cm⁻¹ region of PVDF UHP, uniaxial HP, and biaxial HP, as shown in Fig.6. FTIR is a significant tool for examining the fraction of b-phase content, a-to-b-phase transformation, and the dipole orientation in the PVDF. In general, the characteristic peaks of the a-phase are very easily detected by FTIR absorption because it has vibration bands, such as at 489, 614, 763, 855, and 979 cm⁻¹. Similarly, some previous work reported that the strong peak at 840 cm⁻¹ is a characteristic of the b-phase [21], [28]. Table 3 shows the characteristic absorption bands of each crystalline phase of the samples. By mean FTIR, the quantity of β-phase content in each sample of PVDF can be calculated with equations 3 [28]:

$$F(\beta) = \frac{X_{\beta}}{X_{\alpha} + X_{\beta}} = \frac{A_{\beta}}{(K_{\beta}/K_{\alpha})A_{\alpha} + A_{\beta}} = \frac{A_{\beta}}{(1.26)A_{\alpha} + A_{\beta}} \quad (3)$$

Where $F(\beta)$, represents the β-phase content (%), and $K_{\alpha} = 6.1 \times 10^4$ and $K_{\beta} = 7.7 \times 10^4 \text{ cm}^2/\text{mol}^{-1}$ are the values of absorption coefficients at the respective wavelength of the number range of 763 -1500 cm⁻¹ shown in Fig.6. Where X_{α}, X_{β} is the crystalline mass fraction of α phase and β phase. A_{α} and A_{β} represents the absorption band peaks at 763 and 840 cm⁻¹, as summarized in Table 3. Meanwhile, uni- and biaxial HP have a slightly higher fraction of β-phase than PVDF UHP. It is indicated that high pressing can lead to improving the content of the fraction β-phase.

The increase in β-phase content induced by HP is attributed to the combined effects of thermal activation and compressive stress, which enhance molecular chain mobility and favor the all-trans (TTTT) conformation characteristics of the β-phase. HP has been shown to enable α/γ to β-phase transformation and improve crystallinity by facilitating effective rearrangement of polymer chains under heat and pressure conditions [8], [30]. The higher absorption intensity at 840 cm⁻¹ observed for biaxially HP PVDF reflects an increased density and alignment of polar dipoles, which directly contributes to enhanced piezoelectric performance [8], [21]. This structural evolution provides a clear physical basis for the superior d_{33} values and output voltage response, as improved dipole orientation maximizes charge generation under applied mechanical stress, thereby increasing the sensitivity and efficiency of the piezoelectric device [31].

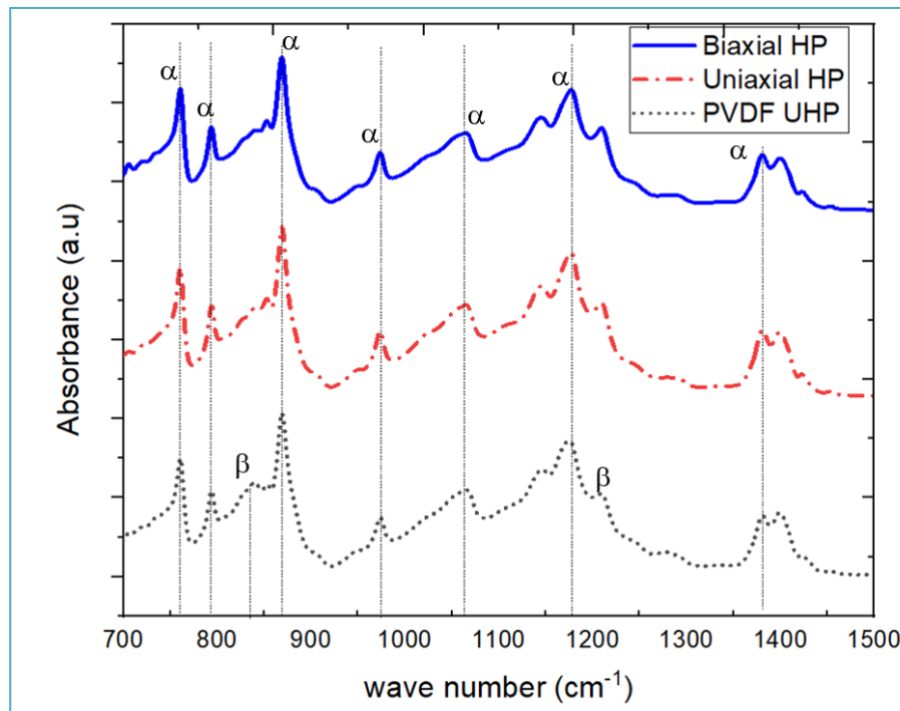


Figure 6. FTIR absorption spectra of PVDF UHP, Uniaxial HP and Biaxial HP

Table 3. The characteristics of FTIR absorption peak of α and β phases of PVDF UHP, Uniaxial HP and Biaxial HP

Hot press method	Wave number (cm ⁻¹)				Fraction of β -phase F β (%)
	α	β	α	β	
	Present Study		Reference [6], [7], [28], [29]		
PVDF UHP	760, 793,		410, 531,	442, 468,	47.80
	869, 973,		615, 763,	510, 600,	
	1064, 1144,	840, 1290	764, 765,	742, 838,	
	1177, 1209,		766, 795,	840, 842,	
	1380, 1400.		796, 854,	849, 880,	
Uniaxial HP	760, 793,		855, 870,	882, 1234,	49.30
	854, 869,		875, 970,	1275, 1278,	
	973, 1064,	840, 1290	976, 1067,	1280, 1290,	
	1145, 1177,		1175, 1210,	1335, 1430	
	1210, 1380, 1401		1215, 1383,		
Biaxial HP	760, 793,		1385, 1402,		50.47
	852, 868,		1430, 1432,		
	973, 1066,	840, 1291	1455		
	1144, 1177,				
	1209, 1380, 1400				

3.3 Output voltage response

The output voltage responses of PVDF UHP, uniaxial HP, and biaxial HP under different impact forces are shown in Fig. 7. Fig. 7(a) shows an example output voltage response of a PVDF film sensor that was recorded for each dropped steel ball using a DSO6034A Agilent digital oscilloscope.

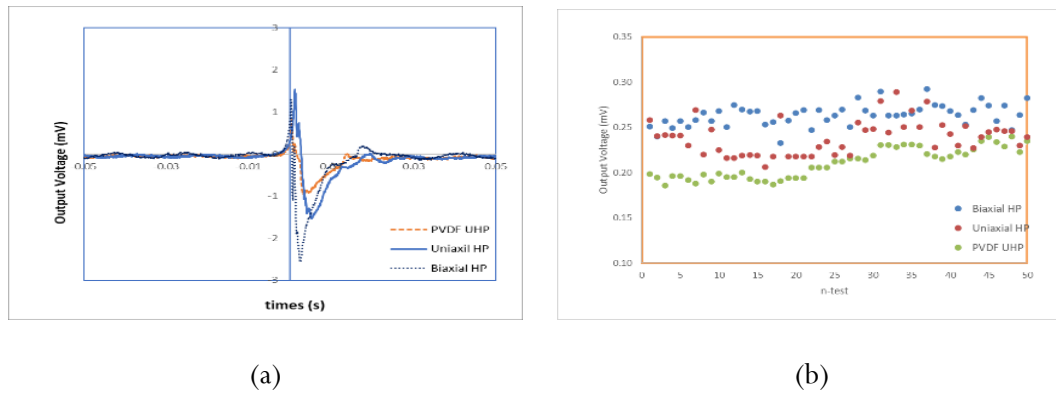


Figure 7. Piezoelectric characterization: (a) Peak-to-peak output voltage response of the PVDF sensor recorded via oscilloscope, and (b) quantitative comparison of the average output voltage across different processing conditions during the impact test

The fluctuating voltage shifts is an important indicator of performance for many PVDF membrane system for sensor, actuator, and energy harvesting. The sensor produces a distinct quasi-AC signal, as shown in Fig. 7(b), where the peak-to-peak (V_{pp}) rises in direct correlation with the impact and release encountered. The impulsive loading phase produces positive voltages, and the unloading phase, also called voltage release, follows with negative peaks. In comparison to uniaxial and standard samples, membranes fabricated with biaxial HP considerably outperform them with a V_{pp} range of 0.1 to 0.35 mV. In addition, after 50 loading-unloading cycles. Biaxial HP samples show minimal signal attenuation, demonstrating superior cyclic stability. It is evident from this resilience that structural relaxation and dipole randomization are greatly reduced, caused by thermomechanically induced crystal stability and molecular alignment acquired by biaxial compression. To enhance the structure-property connection of PVDF, the result demonstrate that biaxial HP is the optimal processing technique. Simultaneously, raising the β -fraction and dipole alignment produces a robust piezoelectric response, which is well suited for sensitive sensing.

3.4 Sensitivity of PVDF film sensor

The important parameter that should be considered in a sensor is sensitivity and accuracy. The sensitivity of the PVDF film sensor is defined as the ratio of the output voltage response (V) to the input impact force F acting on the PVDF, and can be calculated by using the equation [7], [20].

$$\eta = \frac{\text{Output voltage}}{\text{input force}} = \frac{V}{F} \left(\frac{\text{Volt}}{\text{Newton}} \right) \quad (4)$$

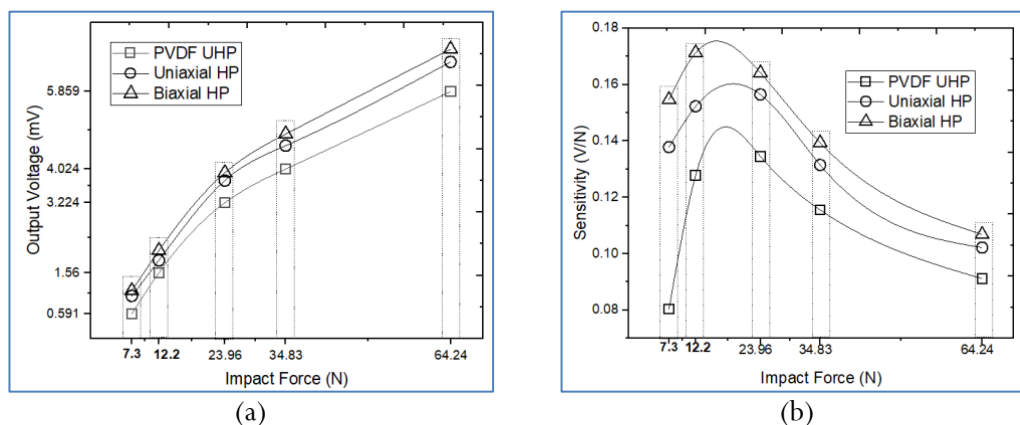


Figure 8. Sensitivity (V/N) Vs Impact force (N)

The responsiveness of the PVDF membrane sensor has been verified by measuring the voltage response to applied impact load. Fig. 8(a) shows that the peak-to-peak output voltage (V_{pp}) exhibits a linear relationship with rising-trend forces, with proportional electromechanical behaviour over the evaluated force range. Furthermore, Fig. 8(b) shows the sensitivity analysis across two regimes. The increase in sensitivity in the lower force range (7.35-12.2 N), and a sustained elevation of sensitivity in the higher force range (23.39-64.24 N). The observations demonstrate that the fabrication membranes exhibit significant responses across a range of forces, especially in low-force applications. Analysis of force-related behaviour shows that mechanical attenuation in thicker PVDF sheets reduces the signal response under increased stress, thereby limiting linearity at higher forces. Conversely, the biaxial HP PVDF showed greater retention of sensitivity under increased applied stress, indicating improved structural stability and resistance to stress-induced depletion. This phenomenon may result from mechanical alterations at the crystalline amorphous interface caused by biaxial HP, which seems to delay the emergence of non-linear electromechanical behaviour and enhance interface strength. Furthermore, the findings indicate that the produced PVDF films are suitable for low-force sensing applications, such as tactile sensors, wearable sensors, and impact monitoring systems. The biaxial HP arrangement exhibits an ideal equilibrium on sensitivity, linearity, and mechanical strength, making it the preferred option for sensitive force-detection applications.

3.5 Piezoelectric properties (d_{33})

Piezoelectric coefficient (d_{33}) measurements from uncompressed PVDF membranes and hot-pressed specimens are shown in Fig.9. The standard deviation results show a gradual increase in d_{33} across the three treatment conditions. The untreated baseline membrane had d_{33} of 17.046 ± 0.065 pC/N, but after uniaxial HP, it elevated to 18.287 ± 0.073 pC/N. The biaxial HP setting produced the strongest piezoelectric response (18.537 ± 0.093 pC/N). In the measurement distributions, the data scatter for baseline and hot-pressed specimens overlaps little, suggesting that the reported improvements are microstructural alterations rather than noise or statistical deviations. Hot-pressings boosts are reproducible and systematic, as seen by the procedure sample separation across repeated measurements. These findings present that HP can improve the PVDF sample's electromechanical response. The thermal and mechanical approach for controlled adjustment of piezoelectric characteristics in membranes is reliable due to the consistency and magnitude of the d_{33} amplification, as well as the non-overlapping measurement distributions.

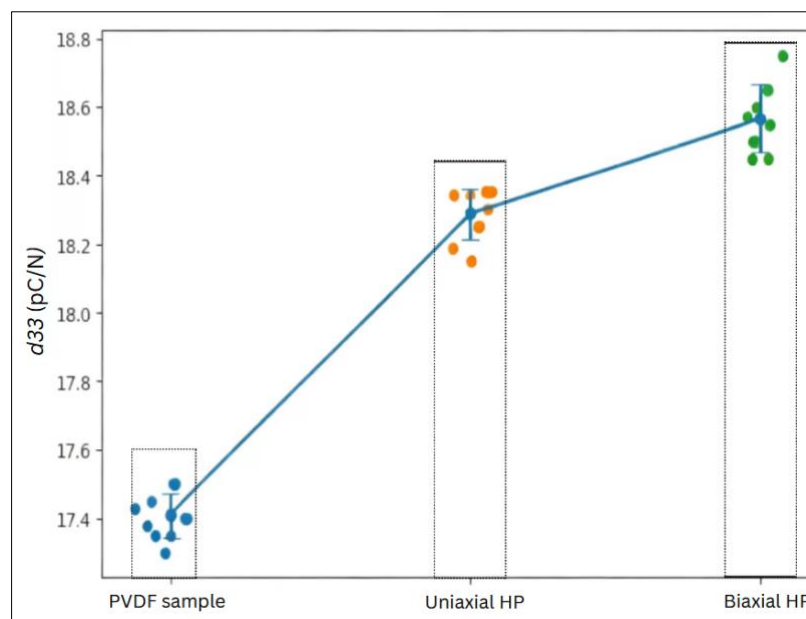


Figure 9. Piezoelectric coefficient (d_{33}) (pC/N)

The found improvement in piezoelectric performance corresponds with recognized structure-property connections in PVDF, where the development and presential orientation of the polar β -phase are the principal factors driving enhanced piezoelectric response [30]. The orientation of molecular dipoles in this crystalline phase is crucial to the sensor's overall electromechanical efficiency. In contrast to uniaxial HP, the biaxial method produces a more isotropic in-plane stress distribution, promoting homogeneous crystalline phase formation and enhanced crystalline consistency across the film thickness. This consistency in microstructural arrangement results in increased functional stability and greater resistance to performance decline under mechanical stress. To put into perspective the insight within the broader literature, Table 4 combines results from leading thermo-mechanical HP studies of PVDF, offering a comparative analysis of essential processing variables, including applied force, processing temperature, and their corresponding effects on the resultant microstructural properties (β -phase fraction, overall crystallinity, and piezoelectric properties). This result provides a basis for the selection of processing parameters used in the current study and shows their conformity with the existing protocols for enhancing the piezoelectricity of PVDF-based devices [18], [26], [32].

Table 4. Hot-pressing of PVDF: Processing parameters and structure–property outcomes

Material/ Method	Applied Force (MPa)	T (°C)	Time (min)	β - Phase (%)	Degree Crystallinity (%)	d_{33} (pC/N)	Ref.
PVDF/HP	0.1	180	180	90	39	13-28	[33]
PVDF/HP	12.25	110- 150	60	82.41	Na	Na	[34]
PVDF (Hot Rolling Press)	5–40	200	120	~97	~47	~30	[27]
PVDF (HP)	50	100	180	~58	12	Na	[8]
PVDF (Folding HP)	20 N	177	Na	~97.5	Na	~20	[35]
PVDF/ZnO HP	2	140– 185	15	Na	42–70	Na	[36]
P(VDF-TrFE)/ HP	10, 20, 30	80- 140	1, 15, 30	66.33	57.86, 62.82, 66.33	Na	[37]
PVDF UHP	60	220	30	47.80	45	17.40	This
Uniaxial HP				49.30	48	18.28	Work
Biaxial HP				50.47	49	18.57	

Furthermore, HP promotes densification by removing voids and microstructural flow sheets present in solution-cast or melt-pressed polymers. This densification mechanism enhances stress transfer between crystalline domains and fortifies electromechanical coupling at the interface, which aligns with previous research highlighting the essential role of microstructural continuity in influencing the piezoelectric performance of PVDF-based systems [8]. The increased d_{33} values found under biaxial HP circumstances can be ascribed to synergistic enhancements in both β -phase fraction, which exhibits an increase of around 3%, a slight alteration that is nonetheless closely related to d_{33} to 18.537 pC/N. This correlation highlights the extent to which microstructural ordering influences piezoelectric output in thermally and mechanically treated PVDF sheets. Moreover, from a practical device standpoint, the recorded peak-to-peak voltage outputs (0.1-0.35 mV) signify a foundational performance appropriate for low-power sensing applications. Although

the values are small, they can be incorporated into device topologies that include signal-conditioning and amplification stages to ensure compatibility with common data acquisition systems and microcontroller input standards.

The biaxial HP processing route offers a significant advantage by enabling the thermomechanical process of dense, avoiding the handling complexities and scalability limitations inherent in solvent-based techniques. The ease of processing offers a significant benefit for industrial applications. In addition, the innovation of this study lies in revealing that biaxial HP can significantly improve the piezoelectric properties of PVDF membranes through mechanical and thermal inputs markedly different from traditional techniques. Although literature indicates that PVDF formulations can achieve β -phase fractions greater than 80%, these outcomes generally result from chemically intensive methods or sophisticated processing equipment, which frequently constrain practical feasibility and longevity. The biaxial HP method examined herein attains a d_{33} of 18.537 pC/N, nearing the efficacy of commercially available stretched film (~ 20 pC/N) [7], while preserving operational simplicity and minimizing solvent-related environmental issues. Nevertheless, the associated enhancement in overall crystallinity (around 4%) is modest, suggesting potential for adding tuning. Future investigations should explore integrated methods to enhance β -phase fractions and consequently improve piezoelectric properties.

4. Conclusion

Overall, this study successfully evaluated how stress distribution affects crystalline phase development in PVDF membranes processed by biaxial HP to improve piezoelectric properties. The results demonstrate that biaxial HP is more effective in promoting the α -to- β -phase and structural order as indicated by an increased β -phase fraction ($F\beta=50.47\%$), and a piezoelectric coefficient ($d_{33}=18.8$ pC/N), quasi-AC signal ($V_{pp}=0.35$ mV), and an increased degree of crystallinity ($X_c=49\%$). These results address a key gap in PVDF membranes processing by providing quantitative evidence that multidirectional stress can improve polymer crystallization. This increase is achieved without solvents or chemical additions using the biaxial HP technique, a thermomechanical alternative to wet-phase routes.

Author's declaration

Author contribution

Suprpto: conceptualization, methodology (PVDF synthesis), supervision, formal analysis, and original composition. **Jubaidah:** investigation and analysis of advanced characterization (XRD and FTIR). **Selamat Triono, Hariyanto Gunawan, Lisyanto, Aditya Sukma Nugraha,** and **Yopan Rahmad Aldori:** curation, investigation, and formal analysis of data, with a particular emphasis on the fabrication, testing, and electrical measurement of PVDF membranes.

Funding statement

This research was funded by the Research and Community Service Institute (LPPM), Universitas Negeri Medan, under the contract number 0250/UN33.8/PPKM/PPT/2025.

Data availability

The data that support the findings of this study are available from the corresponding author upon reasonable request.

Acknowledgements

The authors express their sincere gratitude to the lab workers for their technical assistance during the synthesis and characterization of PVDF membranes. We are profoundly appreciative of the research facilities and resources provided by the Department of Mechanical Engineering at Universitas Negeri Medan and the Research Organization Electronics and Informatics-BRIN, which facilitated the completion of this research. Additionally, we are grateful to the Department of Mechanical Engineering at Chung Yuan Christian University (CYCU), Taiwan, and, in particular, to Professor Ting Yung, for their invaluable assistance and for providing the materials and devices used in this study.

Competing interest

The authors declare that there is no conflict of interest regarding the publication of this paper.

Ethical clearance

Not applicable (this research does not involve human subjects).

AI statement

This article is the original work of the author without using AI tools for writing sentences and/or creating/editing tables and figures in this manuscript. The manuscript underwent professional grammatical review by subject-matter experts to ensure linguistic precision.

Publisher's and Journal's note

Universitas Negeri Padang as the publisher, and Editor of Teknomekanik state that there is no conflict of interest towards this article publication.

References

- [1] L. Wu *et al.*, "Recent advances in the preparation of PVDF-based piezoelectric materials," *Nanotechnology Reviews*, vol. 11, no. 1, pp. 1386-1407, 2022. <https://doi.org/10.1515/ntrev-2022-0082>
- [2] K. Tashiro, H. Tadokoro, and M. Kobayashi, "Structure and piezoelectricity of poly (vinylidene fluoride)," *Ferroelectrics*, vol. 32, no. 1, pp. 167-175, 1981. <https://doi.org/10.1080/00150198108238688>
- [3] Z. Feng *et al.*, "Piezoelectric effect polyvinylidene fluoride (PVDF): from energy harvester to smart skin and electronic textiles," *Advanced Materials Technologies*, vol. 8, no. 14, p. 2300021, 2023. <https://doi.org/10.1002/admt.202300021>
- [4] G. Prasad *et al.*, "Fabrication of intra porous PVDF fibers and their applications for heavy metal removal, oil absorption and piezoelectric sensors," *J Journal of Materiomics*, vol. 9, no. 1, pp. 174-182, 2023. <https://doi.org/10.1016/j.jmat.2022.08.003>
- [5] C. Lee and J. A. Tarbuton, "Polyvinylidene fluoride (PVDF) direct printing for sensors and actuators," *The International Journal of Advanced Manufacturing Technology*, vol. 104, no. 5, pp. 3155-3162, 2019/10/01 2019. <https://doi.org/10.1007/s00170-019-04275-z>
- [6] Y. Ting, Suprpto, A. Nugraha, C.-W. Chiu, and H. Gunawan, "Design and characterization of one-layer PVDF thin film for a 3D force sensor," *Sensors Actuators A: Physical*, vol. 250, pp. 129-137, 2016. <https://doi.org/10.1016/j.sna.2016.09.025>

- [7] Y. Ting, Suprpto, C. W. Chiu, and H. Gunawan, "Characteristic analysis of biaxially stretched PVDF thin films," *Journal of Applied Polymer Science*, vol. 135, no. 36, p. 46677, 2018. <https://doi.org/10.1002/app.46677>
- [8] S. Jang *et al.*, "Studies on phase transformations and crystallinity changes of PVDF thin films via hot-pressing treatment," *Polymer*, vol. 320, p. 128094, 2025. <https://doi.org/10.1016/j.polymer.2025.128094>
- [9] L. Wang, F. Gao, K. Zhang, M. Wang, M. Qin, and J. Kong, "Effect of hot pressing temperature on dielectric and energy storage properties of Ba_{0.6}Sr_{0.4}TiO₃/poly(vinylidene fluoride) composites," *IEEE Transactions on Dielectrics Electrical Insulation*, vol. 24, no. 2, pp. 704-711, 2017. <https://doi.org/10.1109/TDEI.2017.006191>
- [10] Y. Ting, H. Gunawan, A. Sugondo, and C.-W. Chiu, "A new approach of polyvinylidene fluoride (PVDF) poling method for higher electric response," *Ferroelectrics*, vol. 446, no. 1, pp. 28-38, 2013. <https://doi.org/10.1080/00150193.2013.820983>
- [11] L. Ruan, X. Yao, Y. Chang, L. Zhou, G. Qin, and X. Zhang, "Properties and applications of the β phase poly(vinylidene fluoride)," *Polymers*, vol. 10, no. 3, p. 228, 2018. doi: <https://doi.org/10.3390/polym10030228>
- [12] M. Pan, Y. Zhang, and L. Dong, "Fluorophilic interaction-directed crystallization control in PVDF via ultralow fluorinated organic molecule," *Journal of Colloid Interface Science*, p. 139072, 2025. <https://doi.org/10.1016/j.jcis.2025.139072>
- [13] Suprpto *et al.*, "Effect of ITO poling thickness, temperature, and protective layer on piezoelectric PVDF films," *Materials Science in Semiconductor Processing*, vol. 174, p. 108156, 2024. <https://doi.org/10.1016/j.mssp.2024.108156>
- [14] Y. Wang *et al.*, "Effects of stretching on phase transformation of PVDF and its copolymers: A review," *Open Physics*, vol. 21, no. 1, p. 20220255, 2023. <https://doi.org/10.1515/phys-2022-0255>
- [15] M. M. Abolhasani *et al.*, "Porous graphene/poly(vinylidene fluoride) nanofibers for pressure sensing," *Journal of Applied Polymer Science*, 2021. <https://doi.org/10.1002/app.51907>
- [16] D. Rahmadiawan *et al.*, "Enhanced properties of TEMPO-oxidized bacterial cellulose films via eco-friendly non-pressurized hot water vapor treatment for sustainable and smart food packaging," *RSC advances*, vol. 14, no. 40, pp. 29624-29635, 2024. <https://doi.org/10.1039/D4RA06099G>
- [17] Z. De-Qing, W. Da-Wei, Y. Jie, Z. Quan-Liang, W. Zhi-Ying, and C. Mao-Sheng, "Structural and electrical properties of PZT/PVDF piezoelectric nanocomposites prepared by cold-press and hot-press routes," *Chinese Physics Letters*, vol. 25, no. 12, pp. 4410-4413, 2008. <http://10.1088/0256-307X/25/12/063>
- [18] S. Pavithra, S. Moorthy, B. Solomon, and A. Sakunthala, "Influence of preparation techniques on the structural and electrical properties of PVdF-HFP/P123 blend polymer membranes for energy storage applications," *Applied Surface Science Advances*, vol. 20, p. 100583, 2024. <https://doi.org/10.1016/j.apsadv.2024.100583>
- [19] S. Mireja and D. V. Khakhar, "High β -phase PVDF films formed by uniaxial compression," *Polymer*, vol. 293, p. 126665, 2024. <https://doi.org/10.1016/j.polymer.2023.126665>
- [20] Suprpto *et al.*, "Fabrication and characterization of PZT/PVDF composite films for force sensor applications," *Polymer International*, vol. 73, no. 9, pp. 727-747, 2024. <https://doi.org/10.1002/pi.6643>
- [21] X. Cai, T. Lei, D. Sun, and L. Lin, "A critical analysis of the α , β and γ phases in poly(vinylidene fluoride) using FTIR," *RSC advances*, vol. 7, no. 25, pp. 15382-15389, 2017. doi: <https://doi.org/10.1039/C7RA01267E>
- [22] Y. Zhou *et al.*, "Crystallinity and β phase fraction of PVDF in biaxially stretched PVDF/PMMA films," *Polymers*, vol. 13, no. 7, p. 998, 2021. <https://doi.org/10.3390/polym13070998>

- [23] S. Mohammadpourfazeli, S. Arash, A. Ansari, S. Yang, K. Mallick, and R. Bagherzadeh, "Future prospects and recent developments of polyvinylidene fluoride (PVDF) piezoelectric polymer; fabrication methods, structure, and electro-mechanical properties," *RSC advances*, vol. 13, no. 1, pp. 370-387, 2023. <https://doi.org/10.1039/D2RA06774A>
- [24] M. Doumeng *et al.*, "A comparative study of the crystallinity of polyetheretherketone by using density, DSC, XRD, and Raman spectroscopy techniques," *Polymer Testing*, vol. 93, p. 106878, 2021. <https://doi.org/10.1016/j.polymertesting.2020.106878>
- [25] J.-Y. Ren *et al.*, "Enhanced dielectric and ferroelectric properties of poly (vinylidene fluoride) through annealing oriented crystallites under high pressure," *Macromolecules*, vol. 55, no. 6, pp. 2014-2027, 2022. <https://doi.org/10.1021/acs.macromol.1c02436>
- [26] N. Ahbab, S. Naz, T.-B. Xu, and S. Zhang, "A comprehensive review of piezoelectric PVDF polymer fabrications and characteristics," *Micromachines*, vol. 16, no. 4, p. 386, 2025. <https://doi.org/10.3390/mi16040386>
- [27] X. Qi *et al.*, "Processing and characterisation of hot rolling pressed PVDF films with enhanced field-induced polarisation," *Polymer*, vol. 302, p. 127001, 2024. <https://doi.org/10.1016/j.polymer.2024.127001>
- [28] R. Gregorio Jr, "Determination of the α , β , and γ crystalline phases of poly (vinylidene fluoride) films prepared at different conditions," *Journal of applied polymer science*, vol. 100, no. 4, pp. 3272-3279, 2006. <https://doi.org/10.1002/app.23137>
- [29] P. Martins, A. Lopes, and S. Lanceros-Mendez, "Electroactive phases of poly (vinylidene fluoride): Determination, processing and applications," *Progress in polymer science*, vol. 39, no. 4, pp. 683-706, 2014. <https://doi.org/10.1016/j.progpolymsci.2013.07.006>
- [30] H. H. Singh, S. Singh, and N. Khare, "Enhanced β -phase in PVDF polymer nanocomposite and its application for nanogenerator," *Polymers for Advanced Technologies*, vol. 29, no. 1, pp. 143-150, 2018. <https://doi.org/10.1002/pat.4096>
- [31] T. Zhao, Y. Li, and Z. Zhang, "Recent advances in β -phase engineering of PVDF-based piezoelectric composites for enhanced piezoelectricity and wearable applications," *Chemical Communications*, 2026. <https://doi.org/10.1039/d5cc07179h>
- [32] J. Pei, Z. Zhao, X. Li, H. Liu, and R. Li, "Effect of preparation techniques on structural and electrical properties of PZT/PVDF composites," *Materials Express*, vol. 7, no. 3, pp. 180-188, 2017. <https://doi.org/10.1166/mex.2017.1369>
- [33] J.-H. Zhao, B.-S. He, A.-S. Li, C.-N. Wang, Q.-Q. Li, and Z.-J. Hu, "Polar phase formation and piezoelectricity of PVDF by hot-pressing under electrostatic intermolecular interactions," *Chinese Journal of Polymer Science*, vol. 40, no. 7, pp. 799-806, 2022. <https://doi.org/10.1007/s10118-022-2706-4>
- [34] S. P. Muduli, S. Parida, S. Rout, S. Rajput, and M. Kar, "Effect of hot press temperature on β -phase, dielectric and ferroelectric properties of solvent casted Poly (vinylidene fluoride) films," *Materials Research Express*, vol. 6, no. 9, p. 095306, 2019. doi: <https://doi.org/10.1088/2053-1591/ab2d85>
- [35] J. Shen, Y. Zeng, Q. Li, J. Zhou, and W. Chen, "Convenient folding-hot-pressing fabrication and enhanced piezoelectric properties of high β -phase-content poly (vinylidene fluoride) films," *Interdisciplinary Materials*, vol. 3, no. 5, pp. 715-725, 2024. <https://doi.org/10.1002/idm2.12175>
- [36] L. Plesník, K. Čech Barabaszová, S. Holešová, P. Peikertová, G. Simha Martynková, and D. S. Nakonieczny, "Nanocomposite PVDF membrane for battery separator prepared via hot pressing," *Batteries*, vol. 9, no. 8, p. 398, 2023. <https://doi.org/10.3390/batteries9080398>
- [37] J.-H. Bae and S.-H. Chang, "Characterization of an electroactive polymer (PVDF-TrFE) film-type sensor for health monitoring of composite structures," *Composite Structures*, vol. 131, pp. 1090-1098, 2015. <https://doi.org/10.1016/j.compstruct.2015.06.075>

Nomenclature

α -phase	: Non-polar crystalline phase of PVDF
β -phase	: Polar crystalline phase of PVDF (piezoelectric active phase)
d_{33}	: Piezoelectric coefficient (pC/N)
V_{pp}	: Peak-to-peak output voltage (mV)
X_c	: Degree of crystallinity (%)
2θ	: Diffraction angle in XRD (degree)
T	: Temperature ($^{\circ}$ C)
P	: Applied pressure (MPa)
t	: film thickness (mm)
PVDF	: Poly(vinylidene fluoride)
HP	: Hot Pressing
UHP	: Unhot Pressing
FTIR	: Fourier Transform Infrared Spectroscopy
XRD	: X-ray Diffraction
ϵ_r	: relative permittivity
ϵ_o	: permittivity of free space (8.854×10^{-12} F/m)
Q	: generator electric
C	: Capacitance
V	: Output Voltage Response